Modeling Keratoconus Using Induced Pluripotent Stem Cells

Roy Joseph,[1] Om P. Srivastava,[1] and Roswell R. Pfister[2]

[1]Department of Optometry and Vision Science, University of Alabama at Birmingham, Birmingham, Alabama, United States
[2]Eye Research Laboratory, Eye Research Foundation, Birmingham, Alabama, United States

Correspondence: Om P. Srivastava, Department of Vision Sciences, 924 18th Street South, University of Alabama at Birmingham, Birmingham, AL 35294-4390, USA; srivasta@uab.edu.

Submitted: January 8, 2016
Accepted: June 2, 2016

Citation: Joseph R, Srivastava OP, Pfister RR. Modeling keratoconus using induced pluripotent stem cells. *Invest Ophthalmol Vis Sci.* 2016;57:3685–3697. DOI:10.1167/iovs.16-19105

Purpose. To model keratoconus (KC) using induced pluripotent stem cells (iPSC) generated from fibroblasts of both KC and normal human corneal stroma by a viral method.

Methods. Both normal and KC corneal fibroblasts from four human donors were reprogramed directly by delivering reprogramming factors in a single virus using 2A "self-cleaving" peptides, using a single polycistronic lentiviral vector coexpressing four transcription factors (Oct 4, Sox2, Klf4, and Myc) to yield iPSC. These iPS cells were characterized by immunofluorescence detection using of stem cell markers (SSEA4, Oct4, and Sox2). The mRNA sequencing was performed and the datasets were analyzed using ingenuity pathways analysis (IPA) software.

Results. The generated stem cell-like clones expressed the pluripotency markers, SSEA4, Oct4, Sox2, Tra-1-60, and also expressed *pax6*. Our transcriptome analysis showed 4300 genes, which had 2-fold change and 870 genes with a q-value of <0.05 in keratoconus iPSC compared to normal iPSC. One of the genes that showed difference in KC iPSC was *FGFR2* (down-regulated by 2.4 fold), an upstream target of Pi3-Kinase pathway, was further validated in keratoconus corneal sections and also KC iPSC-derived keratocytes (down regulated by 2.0-fold). Both normal and KC-derived keratocytes expressed keratocan, signature marker for keratocytes. KC iPSC-derived keratocytes showed adverse growth and proliferation and was further confirmed by using Ly2924002, a PI3k inhibitor, which severely affected the growth and differentiation in normal iPSC.

Conclusions. Based on our result, we propose a model for KC in which inhibition FGFR2-Pi3-Kinase pathway affects the AKT phosphorylation, and thus affecting the keratocytes survival signals. This inhibition of the survival signals could be a potential mechanism for the KC-specific decreased cell survival and apoptosis of keratocytes.

Keywords: keratoconus, induced pluripotent stem cells, FGFR2, disease modeling

Collagen and extracellular matrix are the essential components of the cornea that maintain its shape and transparency. Keratocytes of the mature cornea are responsible for the production and maintenance of vital corneal components, including extracellular matrices, lumican, and keratocan.[1,2] These interact with collagen fibrils to modulate their size and spacing.[1–3] The causative factor(s) behind the development of keratoconus is not well understood. What is known is that the keratoconus (KC) corneal stroma shows reduced numbers of keratocytes relative to normal corneas.[4,5] This is caused by apoptosis,[6] as evidenced by the upregulation of several apoptotic genes in the keratocytes.[7] The trigger inducing the apoptosis is unknown, but an increased sensitivity of keratocytes to IL-1 after epithelial injury has been suggested as a factor.[8] Keratocytes from both normal and keratoconus, when cultured in the presence of serum, generated cells with phenotypes of fibroblasts, and myofibroblasts, whereas, KC keratocytes when grown in the absence of serum showed poor survivability compared with normal corneal keratocytes.[9] Currently, there is no animal model to assist in the study and understanding of the factors causing this disease.

It is known that embryonic stem cells (ESC) derived from blastocysts have the property to divide indefinitely while maintaining pluripotency[10,11] This capacity of ESC provides an opportunity to understand disease mechanisms, screen a variety of drugs, and treat patients with various injuries and diseases.[12] However, the use of ESC has been limited due to ethical controversies. For this reason, research on induced pluripotent stem cells (iPSC) has gained momentum in recent years. Reprogramming somatic cells to iPSC by the use of classic Yamanaka factors holds great promise for bringing regenerative medicine into a clinical setting.[13] This factor-based reprogramming of adult somatic cells has been generated in mice[14,15] and in humans.[16,17] Induced pluripotent stem cells hold a great promise to identify genetic changes that guide KC disease process. Generating iPSC from adult human somatic cells is a viable alternative for stem cells production. Recently, iPSC generated from swine fetal fibroblasts were differentiated into photoreceptors cells in vitro, and were able to be integrated into damaged neural retina.[18] It has also been shown that iPSC generated from normal human keratocytes could be used to treat corneal injuries[19] and also keratocytes have been differentiated from human ESC (hESC).[20] Experiments designed to explore iPSC, generated from KC fibroblasts, could be of tremendous importance in understanding the disease mechanism. Adult human fibroblasts have been successfully reprogrammed via overexpression of pluripotency-related transcription factors, including OCT4 (POU5F1), SOX2, KLF4, and c-MYC, to establish human iPSC (hiPSC).[21] Several studies have demonstrated close similarities between hiPSC and hESC

at the molecular and genetic levels, which are based on their morphologies and functions.[16,22,23] Disease-specific iPSC lines have also been generated from patients with sporadic or genetically inherited diseases.[17,24–28] Like hESC, iPSC have similar characteristics, allowing them to differentiate into various cell types in response to developmental cues. Recent reports have shown that disease-specific iPSC from spinal muscular atrophy, Friedreich's Ataxia and QT syndrome, were able to successfully recapitulate the disease phenotypes from these disorder.[29–33]

In this study, we have used the iPSC generated from keratocytes of both normal and KC corneas, and performed transcriptome analysis to generate a molecular model for KC. The first objective of this study was to generate iPSC from both normal and KC fibroblasts. In the absence of an animal model for KC, iPSC generated from KC fibroblasts, provide a valuable tool to study the disease at both molecular and genetic levels. The second objective of the study was to analyze the transcriptome changes using RNA sequencing (RNA-Seq) analysis. This high-throughput sequencing-based method has changed the way in which transcriptomes are studied and has many advantages. RNA-Seq directly sequences complementary DNAs (cDNAs) using high-throughput DNA sequencing technologies followed by the mapping of the sequencing reads to the genome. This comprehensive understanding of the complexity of eukaryotic transcriptomes allows for the identification of exons and introns, identification of transcription start sites,[34] and also the identification of new splicing variants. Additionally, it allows for the precise quantification of exon expression and splicing variants.[35–40]

Methods

Human Cornea

Corneas from KC patients were recovered within 1 to 2 hours following surgery. Deep anterior lamellar keratoplasty, using the "big bubble" technique, removed the full thickness of corneal stroma from six individuals and six age-matched normal corneas were used for this study. Each cornea was placed in Optisol, (Chiron Ophthalmics, Irvine, CA, USA) and refrigerated within 15 minutes. Studies were initiated within 1 hour. Only the epithelium needed to be removed because the endothelium was not present in the specimen. Age-matched normal and healthy corneas that were suitable for transplantation, stored in Optisol at 4°C by the Alabama Eye Bank (Birmingham, AL, USA), were obtained within 12 hours after their enucleation. These normal corneas were fit for corneal transplantation but did not meet the criteria because of plasma dilution so could not run the serologic test. But otherwise these corneas were healthy enough for transplantation. A central 8-mm trephination was performed. The epithelium and endothelium were gently scraped off, leaving the stroma to be used in these experiments. Four normal corneas from the Eye bank, (58- [identified as N1] and 38-year-old females [N4], and 54- [N2] and 59-year-old males [N3]), and four age-matched KC corneas (41- [K1] and 35-year-old females [K4], and 31- (K2) and 44-year-old males [K3]) were used for generating corneal fibroblasts cultures and two KC (39-year-old female [K5] and 64-year-old male [K6], and two age-matched normal 48-year-old female [N5] and 72-year-old male [N6]), were used for immunohistochemical analysis. All six individuals entered into this study had a long history of severe KC with resulting poor vision and a history of contact lens failure (details provided as Supplementary Data S1). Their topography revealed a central keratometry of 61.5 to 96.5 diopters (D), with scarring over the apex. A corneal transplant offered their only chance for improved visual acuity. The procurement of human corneas in this study was approved by the institutional review board of the University of Alabama at Birmingham (Birmingham, AL, USA), following the tenets of the Declaration of Helsinki for Research Involving Human Subjects.

Viral Preparation

To generate FUW-SOKM-harboring lentiviruses (LvSOKM),[41] HEK-293 cells (3×10^6 cells per 10-cm dish) were cotransfected with a mix of 10 μg of pMD2.G plasmid encoding the vesicular stomatitis virus glycoprotein (VSV-G) envelop, 10 μg of psPAX2 packaging plasmid, and 12 μg of the FUW-SOKM (Addgene plasmid 20325; Addgene, Cambridge, MA, USA), a lentiviral Sox2-P2A-OCT4-T2A-Klf4-E2A-cMyc-harboring shuttle, using lipofectamine 2000 (Invitrogen, Grand Island, NY, USA) according to the manufacturer's instruction. The media was changed to Dulbecco's modified Eagle's medium (DMEM; Invitrogen) after 24 hours. The next day, the supernatant was collected, centrifuged at 805*g* for 5 minutes to remove cellular debris, filtered through a 0.45-μM filter (Whatman cellulose filter paper; Sigma-Aldrich Corp., St. Louis, MO, USA), and concentrated by ultrafiltration. The virus pellets were resuspended in DMEM/F12 containing 10% fetal bovine serum (FBS).

Cell Culture and Viral Infection of Stromal Fibroblasts

Four individual cultures were generated from both normal (N1, N2, N3, and N4) and KC (K1, K2, K3, and K4) corneas, and all the experiments were done in triplicate. Primary cultures of human corneal fibroblasts were established as described earlier[11] and passage two was used for this study. The corneal stromal fibroblasts from four normal and four KC corneas (passage 2) were infected in a 6-well plate (Corning, Tewksbury, MA, USA) by 1×10^6 LvSOKM particles with multiplicity of infection (MOI) = 10, diluted in 2 mL of DMEM/F12 medium supplemented with 10% FBS (Hyclone, Logan, UT, USA) and polybrene (8 μg/mL; Sigma-Aldrich Corp.). The cells were reinfected after 24 hours with virus particles as described above. The cells were trypsinized and cultured in TeSR-E7 media (StemCell Technologies, Inc., Vancouver, Canada) for 6 days with regular change of media and followed by mTeSR1 media (StemCell Technologies, Inc.). After 21 days, the individual hES-like clones were manually picked using a sterile tip and transferred to low attachment plates for 5 days in mTeSR1 media (StemCell Technologies, Inc.). The ES-like clones were dissociated using enzyme-free cell dissociation reagent (StemCell Technologies, Inc.), and the ES-like clones were analyzed for stem cell markers.

Immunofluorescence Imaging

The stem cell–like clones from both normal and keratoconus corneas were identified under a microscope, and were recognized according earlier published data.[41] These clones were removed manually using sterile pipette tips under an inverted microscope, seeded on to 18-mm glass cover slips, fixed with 4% formaldehyde for 30 minutes at room temperature, and washed 3× with PBS. The cells were then incubated with a blocking solution containing 10% normal serum and 0.5% BSA in PBS for 1 hour, followed by incubation with a primary antibody at 4°C for 24 hours. The following individual primary antibodies were used: Tra-1-60 (mouse mAB, 1:1000), Sox2 (rabbit mAB, dilution 1:400), SSEA4 (mouse mAB, 1:500), and Oct4 (rabbit mAB, dilution 1:400) (Cell Signaling, Danvers, MA, USA). The cells were washed three times in PBS, followed by incubation with a secondary antibody for 1 hour in the dark (Invitrogen) with the following secondary antibodies (goat anti-rabbit IgG-AlexaFluor 488 conjugate, dilution 1:1000) and goat anti-mouse IgG-AlexaFluor

Investigative Ophthalmology & Visual Science

594 conjugate, dilution 1:1000). The cells were washed again three times in PBS, and incubated with Hoechst nuclear stain for 10 minutes, washed again in PBS, and mounted on to glass slides with a mounting medium (Fluoromount-G; Southern Biotech, Birmingham, AL, USA). Mouse IgG was used as a negative control with the identical protein concentration as that of the primary antibodies.

RNA Isolation and RNA Sequencing

RNA was extracted with Trizol reagent (Invitrogen) from 100 randomly selected iPSC clones from (N3), and (K2 and K4) KC iPSC, respectively, and all the samples were done in duplicates. The mRNA sequencing was performed at the Genomics Core Laboratory of University of Alabama at Birmingham. Analysis was carried out on the Illumina HiSeq2500 (paired end 2×50 bp sequencing runs; Illumina, San Diego, CA, USA). The quality of the total RNA isolated from iPSC clones of both normal and KC corneas was assessed using the Agilent 2100 Bioanalyzer (Agilent Technologies, Santa Clara, CA, USA) followed by two rounds of poly A^+ selection and conversion to cDNAs. The samples were DNAse treated and 800 ng of total RNA was used to making the libraries. The TruSeq library generation kits were used according to the manufacturer's instructions (Illumina). Library construction consisted of random fragmentation of the polyA mRNA followed by cDNA production using random primers. The ends of the cDNA were repaired, A-tailed, and adaptors ligated for indexing (up to 12 different barcodes per lane) during the sequencing runs. The cDNA libraries were quantified using qPCR in a Roche LightCycler 480 (Roche Diagnostics, Indianapolis, IN, USA) with the Kapa Biosystems kit for library quantification (Kapa Biosystems, Woburn, MA, USA) prior to cluster generation. Approximately 725 to 825 K clusters/mm were generated.[35] Cluster density and quality was determined during the run after the first base addition. The raw data files were then converted to the fastq file format using Illumina's bcl2fastq version 1.8.4. TopHat version 2.0.12 was used to align the raw RNA-Seq fastq reads to the human hg19 reference genome using the short read aligner Bowtie.[42–44] TopHat also analyzes the mapping results to identify splice junctions between exons. Cufflinks version 2.2.1 was used to align the reads from TopHat to assemble transcripts, estimate their abundances, and test for differential expression and regulation.[44,45] Cuffmerge, which is part of Cufflinks, merged the assembled transcripts to a reference annotation and is capable of tracking Cufflinks transcripts across multiple experiments. Cuffdiff found significant changes in transcript expression, splicing, and promoter use. The datasets were analyzed using ingenuity pathways analysis (IPA) software (Ingenuity Systems, Redwood City, CA, USA). The IPA was done for all the genes that had a fold change greater than or equal to ± 2, q value less than 0.05.

Reverse Transcription-Quantitative Polymerase Chain Reaction (RT-PCR [qPCR])

Real-time PCR quantifications were performed using the BIO-RAD iCycler iQ system (Bio-Rad, Hercules, CA, USA), in a 96-well reaction plate for a total volume of 25 μL. RNA was extracted as described above. Primers were designed using Primer3 for the following genes: *Sox2*, *Pax6, KERA*, and *GAPDH* and the primers are described in Supplementary Table S1. The reaction mixture included 12.5 μL of Real-Time SYBR Green PCR master mix, 2.5 μL of reverse transcription product, 1 μL of forward and reverse primer, and 8 μL of DNase/RNase free water. The reaction mixtures were initially heated to 95°C for 10 minutes to activate the polymerase, followed by 40 cycles, which consisted of a denaturation step at 95°C for 15 seconds, annealing at 57°C for 60 seconds, and elongation step at 72°C. The qRT-PCR data were analyzed by the comparative ΔCt method.

Differentiation of iPSC to Keratocytes

The undifferentiated iPSC clones from three KC and three normal corneas were separated as described above and clones were grown in low attachment culture plates (Sigma-Aldrich Corp.) for 5 days in the presence of Tesr1 media to form Embryoid Body (EB). Next, 30 to 50 clones were removed, and were plated on 0.1% matrigel-coated (Sigma-Aldrich Corp.) 6-well plates in the presence of modified keratocyte differentiation of iPSC to keratocytes (DMEM/F12, 10 ng/m FGF2, insulin [1.0 mg/mL], transferrin [0.55 mg/mL], and selenite [0.5 μg/mL] (ITS); Sigma-Aldrich Corp.). The medium was changed every 2 days and the iPSC differentiation was analyzed using an inverted light microscope with images taken at the time of seeding depicted as day 1, followed by images taken on the seventh day. The cells were counted from each pictograph from both three normal and three KC, and was plotted on an excel sheet. The RNA was isolated from differentiated cells from normal and KC iPSC for qRT PCR analysis and was performed as described above.

Immunohistochemical Analysis of *FGFR2* Expression

The immunohistochemistry for *FGFR2* (rabbit polyclonal FGFR2 antibody, dilution 1:500; Abcam, Cambridge, MA, USA) expression in corneal tissue were done according to procedure described earlier,[11] and similarly the *FGFR2* expression in differentiated cells was determined as described earlier.[46]

Inhibition of Pi3 Kinase

Pi3 kinase was inhibited in 50 undifferentiated normal stem cell clones by treatment with 10 μM Ly292004 (Sigma-Aldrich Corp.) in the presence of keratocyte differentiating media. The isolation and maintenance of normal iPSC clones were done as described above. The effects of PI3 kinase inhibition were studied for 24 hours as described above in the Methods section. Normal iPSC were differentiated in the absence of Ly292004.

Statistical Analysis

The statistical significance was determined by Student's *t*-test and with statistical significance set at P less than 0.05 and also q value with statistical significance set at q less than 0.05.

Results

Generation of iPSC From Normal and Keratoconus Corneal Fibroblasts

Forced expressions of the transcription factors, Oct4, Sox2, Klf4, and c-Myc (Fig. 1A) in normal and KC fibroblasts (Figs. 1B, 1D), induced the formation of cell colonies that were similar to embryonic stem-like clones in appearance (Figs. 1C, 1E). These stem cell–like colonies were fully formed after 21 days post induction. Our phase-contrast microscopic images of iPSC from both KC and normal corneas showed more than 25 hESC-like colonies per 10^5 cells (Figs. 1C, 1E). The clones were analyzed for stem cell markers as described in the Methods section. Immunocytochemical analysis revealed that these stem cell–like colonies expressed pluripotency markers Tra-1-60/Sox2 in both stem cell–like colonies generated from normal and KC corneas

Investigative Ophthalmology & Visual Science

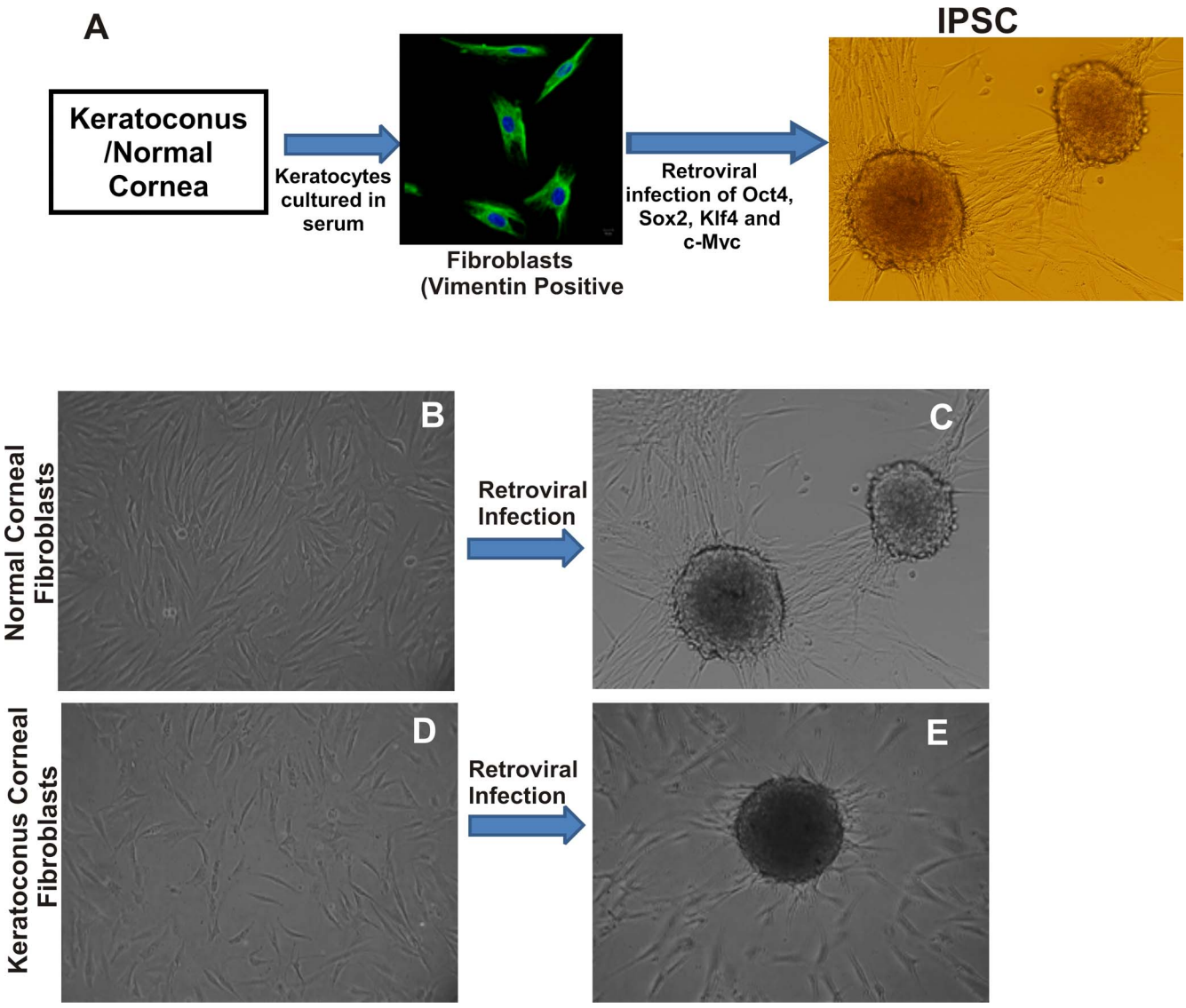

Figure 1. (**A**) Experimental strategy used for reprogramming the corneal fibroblasts. (**B–E**) Generation of iPSC from fibroblasts of KC and normal corneal stroma. (**B**) Normal corneal fibroblasts from a cornea of a 54-year-old male donor before treatment with lentiviral vector. (**C**) Stem cell–like clones developed from normal corneal fibroblasts after 21 days (25 clones were seen per 10^5 adult cells). (**D**) Keratoconus corneal fibroblasts from a cornea of a 44-year-old male donor before lentiviral treatment. (**E**) Stem cell–like clones developed in KC fibroblasts after 21 days (25 clones were seen per 10^5 adult cells).

(Figs. 2A, 2B). These colonies also expressed the pluripotency marker SSEA4/Oct4 (Figs. 2C, 2E). We also analyzed for *Sox2* and *PAX6* expression in keratoconus clones. For the expression analysis, RNA was isolated (as described in the Methods section) from stem cell clones generated from KC and were compared with the fibroblasts cells generated from both normal and keratoconus. Both *Sox2* and *Pax6* were upregulated in KC iPSC compared with fibroblasts cells (Fig. 2E).

RNA-Seq Analysis

High-throughput cDNA sequencing (RNA-Seq) can identify genes and splice variants and also quantify expression in a single assay.[35,37,45] The RNA quality analysis showed it to be of high quality, and RNA integrity number (RIN) for all samples was 9.5 or greater. The read alignment with TopHat for the all samples is provided as supplementary data (Supplementary Table S2). A total of 28,665 genes were analyzed by RNA-Seq (Supplementary Table S3), and of these 4300 genes showed greater than or equal ±2-fold change and 870 genes with q value less than 0.05 in KC compared with normal iPSC (Supplementary Table S4). There were 208 genes that showed infinity (expressed either in KC or normal); most notable were *MIR100* and *MIR186*. The major genes that showed differences were *COL5A1*, *FGFR2*, *EZR*, *DPYSL4*, *MMP9*, *TGFBRIII*, *COL4A1*, *COL4A2*, *IL6*, *SFRP1*, and *HGF*. The datasets were analyzed using IPA, which revealed genes affected were connected to several pathways, mainly to growth and proliferation, cell survival, cell cycle, cancer, and several others (Fig. 3). One of the genes affected was *FGFR2*, which was downregulated by 2.4 (Log2)-fold, as well as the downstream targets that it affects (Fig. 4).

Differentiation of Keratocytes From Both Normal and KC iPSC

The stem cells clones were isolated and were cultured in keratocyte differentiating media as described in the Methods

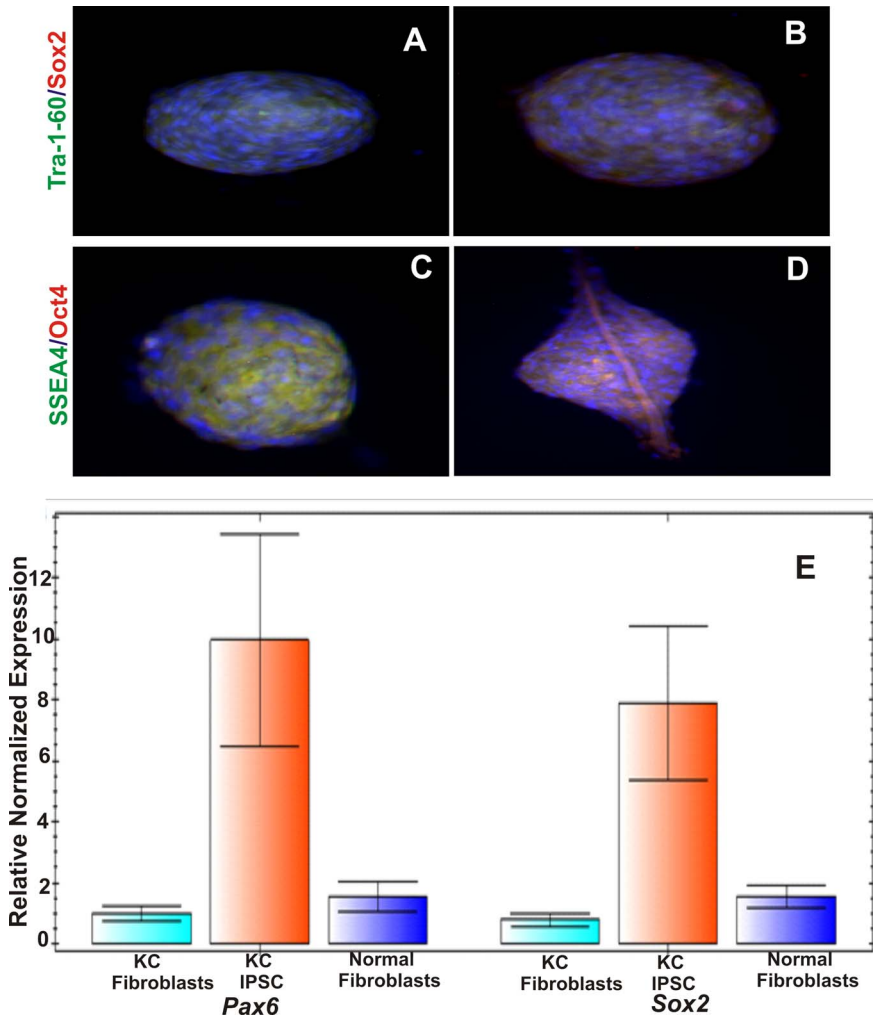

Figure 2. Examination of stem cell markers in iPSC generated from KC and normal corneal fibroblasts. (**A–D**) Immunocytochemical analysis of stem cell markers (TRA1-60 [*green*], Sox2 [*red*], SSEA4 [*green*], and Oct4 [*red*]). (**A**) An overlay of TRA-1-60, SOX2, and nuclear stain in stem cell–like clones from normal cornea. (**B**) An overlay of TRA-1-60, SOX2, and nuclear stain in stem cell–like clones from KC cornea. (**C**) An overlay of SSEA4, Oct-4, and nuclear stain in stem cell–like clones from normal cornea. (**D**) An overlay of SSEA4, Oct-4, and nuclear stain in stem cell–like clones from KC cornea. (**E**) Quantitative RT-PCR analysis of stem cell marker (*SOX2* and *PAX6*) in stem cell–like clones from KC.

section. The differentiated cells are shown in Figures 5B and 5D from the normal and KC iPSC, respectively. The RNA was isolated from cells differentiated from both normal and KC iPSC and was reverse transcribed as described in the Methods section. Reverse-transcription PCR analysis of the RNA was done (Figs. 5E, 5F) using keratocan as a marker for corneal keratocytes.

Expression of *FGFR2*

Our RNA-Seq analysis results showed that *FGFR2* expression was −2.4 (log2-fold change) decreased in the stem cells that were generated from fibroblasts of KC compared with stem cells from normal corneas. Immunohistochemical analysis of *FGFR2* expression was decreased in stromal keratocytes and epithelial sections of KC corneas compared with normal corneas (Figs. 6A, 6B). We also analyzed the expression of *FGFR2* in keratocytes that were differentiated from normal and KC iPSC (Figs. 6C, 6D, respectively) using immunocytochemical analysis as described as in the Methods section. The FGFR2 expression levels were decreased in KC iPSC-derived keratocytes compared with that of the normal iPSC. We further analyzed the pixel intensity in $n = 22$ cells from both types of differentiated cells using ImageJ software (http://imagej.nih.gov/ij/; provided in the public domain by the National Institutes of Health, Bethesda, MD, USA) as described earlier.[46] The *FGFR2* expression levels were decreased by 2-fold in keratocytes differentiated from KC (Fig. 6E).

Proliferation of Keratocytes Generated From iPSC

Stem cells were differentiated from both normal and KC corneas as described in the Methods section. Figures 7A, 7C, and 7E, show iPSC generated from three different normal corneas (N1, N2, and N3) in the presence of differentiation media at day 1 and Figures 7B, 7D, and 7F show keratocyte differentiation after 7 days. Similarly, Figures 7G, 7I, and7K show iPSC generated from three different KC (K1, K2, and K3) and Figures 7H, 7J, and 7L show keratocyte differentiation after 7 days. The cells differentiated from KC iPSC had fewer numbers of cells compared with those differentiated from the normal iPSC (Figs. 7H, 7J, and 7L compared with 7B, 7D, and 7F). The differentiated cells were counted as described in the Methods section (Fig. 7M), shows that number of cells was decreased in cells differentiated from KC iPSC compared with

Investigative Ophthalmology & Visual Science

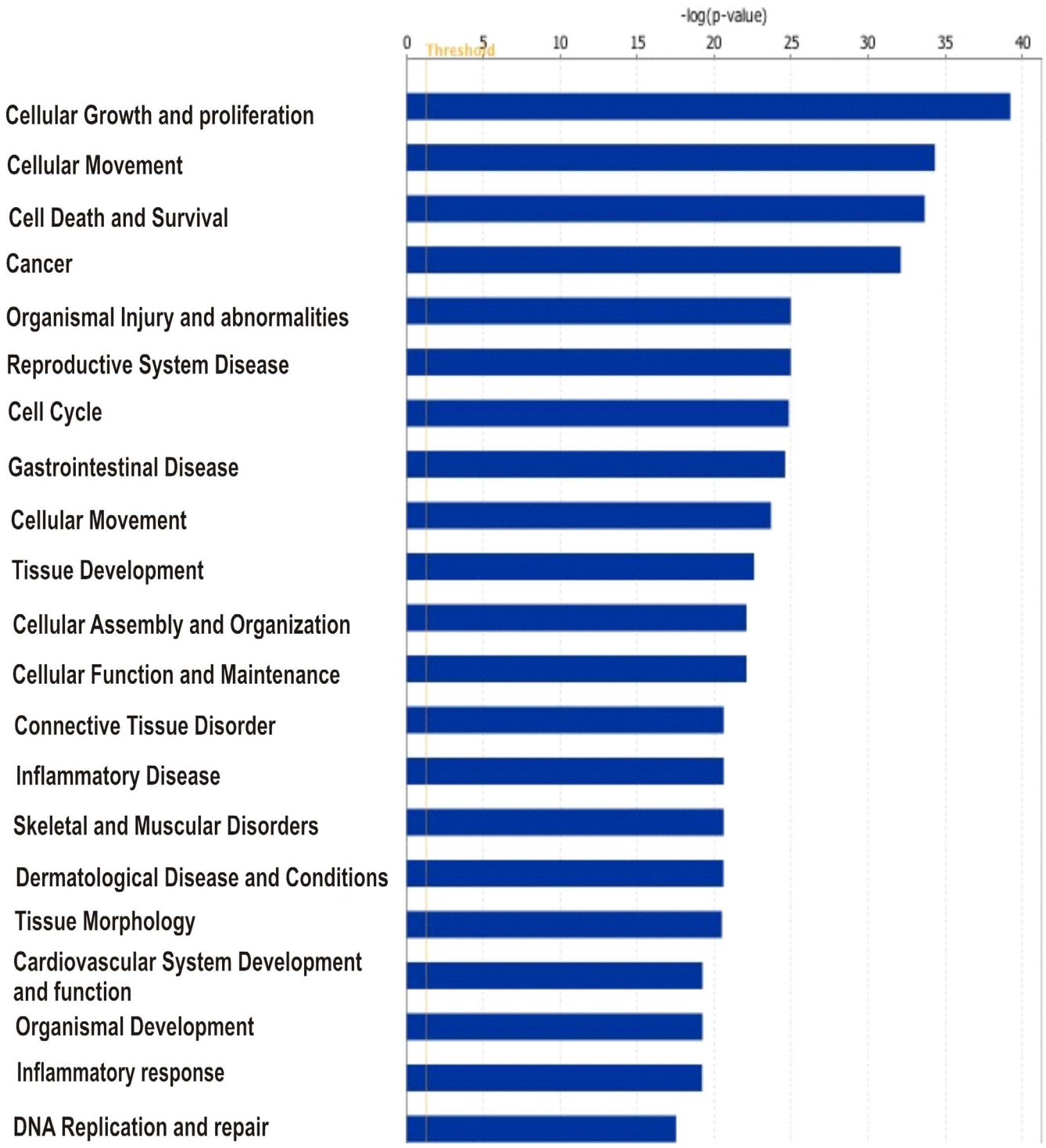

Figure 3. Ingenuity pathway analysis of genes that showed fold changes ($\geq \pm$ 2-fold and q value < 0.05) in iPSC of normal compared with KC corneas. Ingenuity pathway analysis revealed genes connected to growth factor signaling biology mainly cellular growth and proliferation, cellular movement and cell death and survival were affected during KC.

normal. We speculate that proliferation and migration of cells were adversely affected in KC iPSC-derived keratocytes compared with similar cells from normal corneal iPSC. Our previous results had shown that an inhibition of Pi3-Kinase (Pi3K) affected the migration and proliferation of normal corneal fibroblasts, similar to their treatment with β-actin siRNA.[46] Pi3-Kinase is a downstream target of the FGF and the IGF pathways and effects both cell proliferation and growth. We used the phosphatidyl-inositol 3-kinase (PI3K) inhibitor Ly2924002 to determine if inhibition of the FGF pathway leads to inhibition of both proliferation and differentiation of iPSC. Figures 7N and 7O show the effects of PI3K inhibition on keratocytes that were differentiated from normal iPSC in the absence and presence of the inhibitor, respectively.

Investigative Ophthalmology & Visual Science

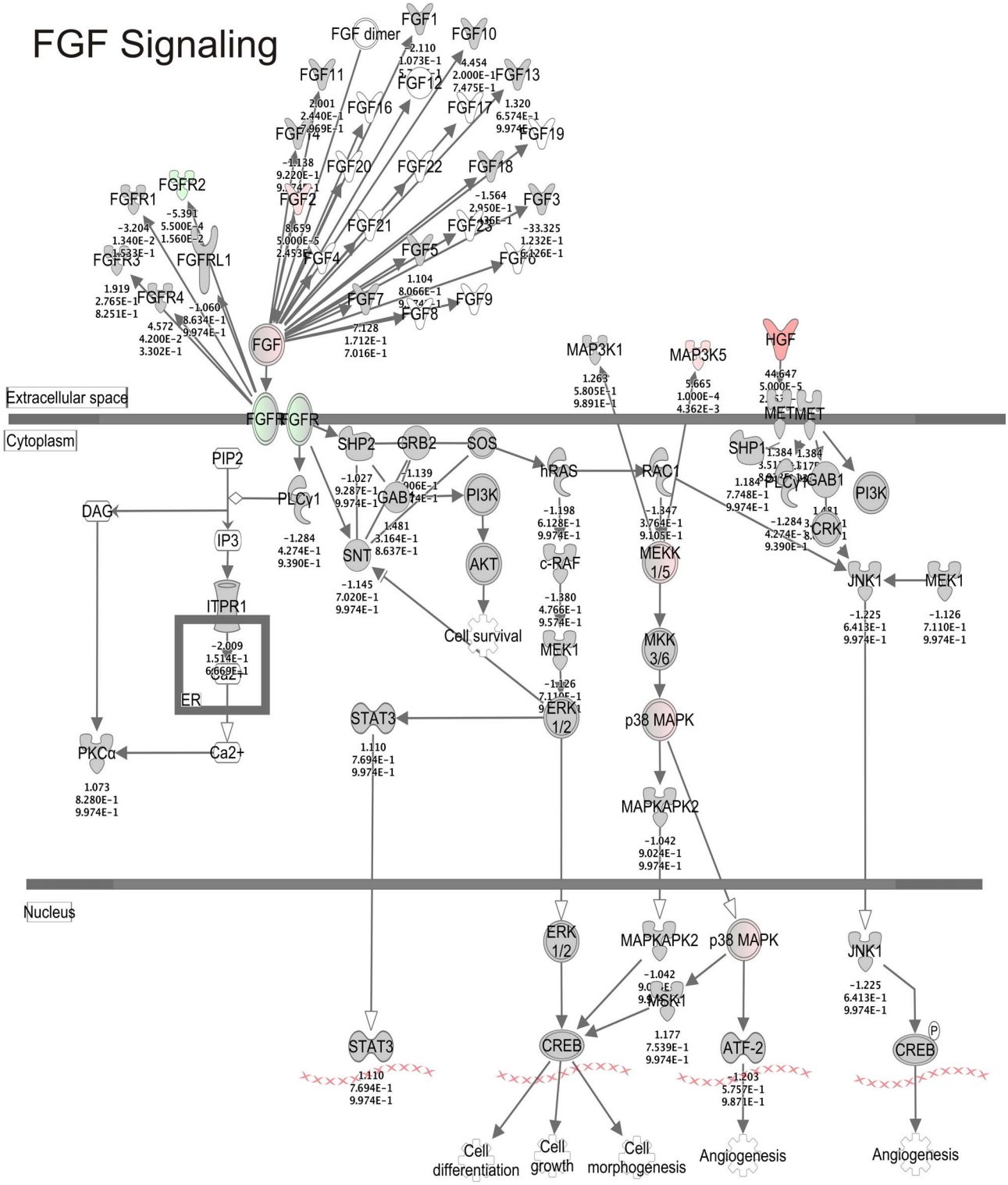

Figure 4. Fibroblast growth factor receptors and genes that are involved in FGF pathway were analyzed by IPA in KC iPSC compared with normal iPSC. The genes that are upregulated or downregulated are shown. Fibroblast growth factor signal transduction. Formation of the FGF:FGFR:HS signaling complex causes the activation of the intracellular kinase domains and the cross-phosphorylation of tyrosines on the FGFRs. FRS2 interacts with the phosphorylated tyrosines and is phosphorylated itself. FRS2 then activates the adaptor protein Grb2 that associates with SOS, a nucleotide exchange factor that activates Ras. Ras is a small GTP binding protein that activates Raf, which activates MEK and that activates ERK, the downstream targets are the cell differentiation, cell growth, and morphogenesis. FRS2 activity also activates phosphoinositide-3 kinase, which activates AKT/PKB and it affects cell survival. PLCγ binds the actvated FGFR by its SH2 domain and then generates inositol-1,4,5-trisphosphate and DAG from phosphotidylinositol-4,5-diphosphate resulting in the activation of protein kinase C and the release of intracellular calcium. The downstream targets also affect angiogenesis, which are through the JNK and p38MAPK.

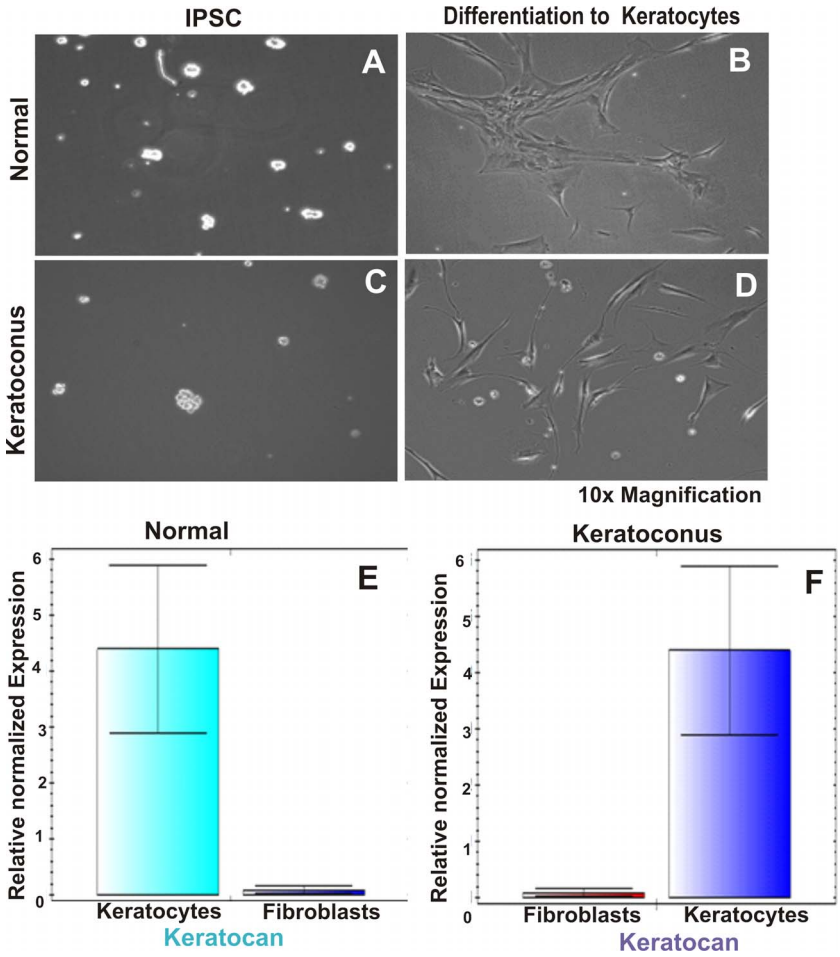

Figure 5. Analysis of corneal differentiation of iPSC to keratocytes. (**A**, **C**) Phase contrast image of iPSC clones from normal and KC, respectively. (**B**, **D**) Differentiated keratocytes from normal and KC, respectively. (**E**, **F**) Quantitative RT-PCR analysis of keratocan gene as a keratocyte marker. (**E**) RNA was isolated and qRT-PCR analysis of keratocan expression in normal iPSC-derived keratocyte. (**F**) Keratocan expression in KC iPSC-derived keratocytes.

Discussion

Generation of patient-derived pluripotent stem cells (PSC) by somatic cell nuclear transfer (NT) has not been successful. However, directly reprograming human somatic cells to produce iPSC by introducing a set of transcription factors linked to pluripotency has been successful.[47] These types of cells overcome the impediments of using animal models, where human diseases have limited representation. In the last 3 years, over a hundred reports have been generated using disease-specific iPSC,[17,24] including polygenic diseases such as Parkinson's,[48] and Alzheimer's,[49–51] and schizophrenia.[52]

We have, for the first time, generated cultures of iPSC from fibroblasts of KC and from normal corneas by both viral and nonviral methods (Joseph R, et al. *IOVS* 2014;55:ARVO E-Abstract 523). Our phase-contrast microscopic images of iPSC from both normal and KC corneal fibroblasts showed good embryonic, stem cell–like clones (Figs. 1C, 1E), and the stem cell–like clones were positive for each of the pluripotency markers. The advantage of reprogramming somatic cells to iPSC is the ability to reset the cellular identity back to the embryonic state, thus enabling studies of complex diseases such as KC. This genetic reprogramming was achieved by ectopic expression of four transcription factors (Oct4, Sox2, Klf4, and c-Myc) using either nonviral or retroviral methodology.[53]

A wealth of new data from studies of the epigenome, genome transcriptome, proteome, and metabolome analyses has led to the consensus that iPSC and ESCs are similar, and these iPSC harbor the molecular memory of their past.[54] It is debatable whether subculturing iPSC induces mutation over time.[55] To rule out this possibility, we have performed RNA-Seq analyses on both KC and normal corneal iPSC, without subculturing, so that mutations are not introduced under culture conditions. As stated above, in recent years transcriptome profiling by next-generation sequencing (RNA-Seq) has significantly improved the study of gene expression.[56] Using RNA-Seq, we have provided, for the first time, a comprehensive assessment of the genes that are regulated in iPSC derived from KC fibroblasts compared with in iPSC derived from normal corneal fibroblasts. Our data show that KC iPSC exhibited significant downregulation of genes that were involved in cell proliferation, differentiation, cell cycle, and in cancer (aberrant cell proliferation; Fig. 3). Our RNA-Seq data also showed that *FGFR2* was downregulated by 2.4-fold (Log2) in KC iPSC compared with normal corneal iPSC (Fig. 4). Further, it showed a reduction in the expression of collagen genes, actin binding protein (*EZR*), and *ACTB*,[11] as has been reported previously. In this regard, it has been shown that *COL5A1* has a single nucleotide polymorphism (SNP), suggested to be involved in corneal thinning in KC.[57]

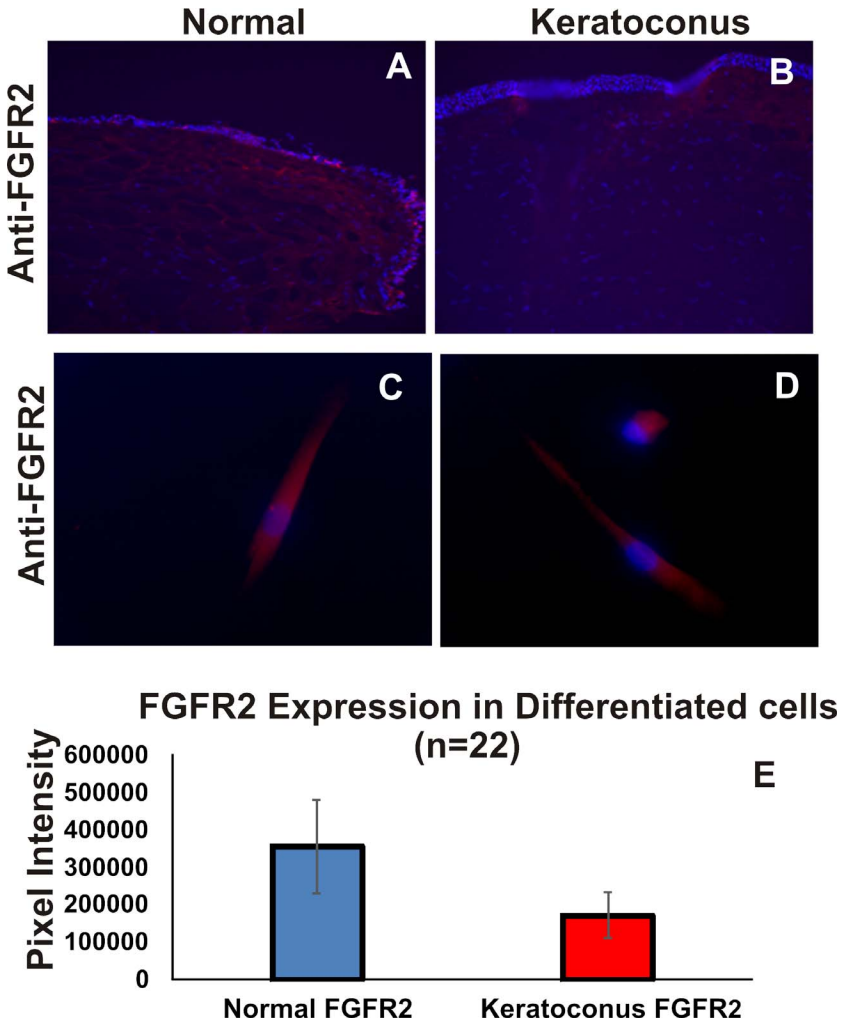

Figure 6. Immunohistochemical analysis of FGFR2 expression in KC and normal corneal sections. (**A**) An overlay of both anti-FGFR2 (*red*) and nuclear stain (*blue*) in normal corneal section. (**B**) An overlay of both anti-FGFR2 (*red*) and nuclear stain (*blue*) in KC corneal section. (**C**) Fibroblast growth factor receptor 2 expression in keratocytes differentiated from iPSC. (**C**) Overlay of both anti-FGFR2 (*red*) and nuclear stain (*blue*) in keratocytes differentiated from normal corneal iPSC. (**D**) Same overlay as in (**C**) but in keratocytes differentiated from KC iPSC. (**E**) Fibroblast growth factor receptor 2 expression in iPSC-derived keratocytes and quantified by ImageJ from both normal and KC ($n = 22$). Fibroblast growth factor receptor 2 expression was downregulated by approximately 2-fold.

A variety of enzymatic and genetic changes were found during the course of this study. *TGFBRIII* was upregulated in KC-iPSC (Supplementary Table S1). *TGFBRIII* inhibits proliferation and migration, and is downregulated in most types of cancers.[58,59] The phosphorylation of *EZR* is important for the survival of epithelial cells through the activation of the PI3K/AKT pathway. *EZR* binds to p85 (a regulatory subunit of PI3K) in three-dimensional (3D) cell cultures of the epithelial cell line LLC-PK1.[60] Our data also showed that 4300 genes showed greater than or equal to ±2-fold change and 870 genes with q value less than 0.05 in KC compared with normal iPSC. Polo-like-kinase 1 (*PlK1*) was also downregulated in KC-iPSC compared with normal corneal iPSC (Supplementary Table S1), and is involved in the cell cycle regulation.[61] Genes that showed changes in genome-wide association and other KC studies were also seen in the RNA-Seq analysis (Supplementary Tables S2, S3), and were: *COL5A1*,[57] *FOXO1*,[62] *HGF*,[63] *LOXL2*,[64] *IL6*,[65] and *SFRP1*.[66] Because it is known that iPSC carry molecular memory, the gene expression analysis by RNA-Seq on these iPSC would enable us to generate a molecular model for KC. Our expression analysis showed major changes in genes that are involved in cell proliferation and cell cycle, leading us to focus on one specific gene, *FGFR2*.

Fibroblast growth factor receptor, a tyrosine kinase receptor, activates the signal transduction pathways, which is mediated through the Pi3K/AKT-signaling pathway. It is known that the PI3K/AKT pathway delivers an antiapoptotic signal.[67] It has been shown that FGFR2, and its ligand FGF, are expressed in the corneal keratocytes.[68] Recently, it has been shown that FGFR2 knockout mice showed a thinner cornea and also an absence of keratocan expression.[69] Keratocan is a marker for keratocytes, suggesting that differentiation of keratocytes was disrupted.[69] Our immunohistochemical analysis of KC corneas also showed a reduced expression of FGFR2 compared with normal cornea (Fig. 5B). In addition, our immunocytochemical analysis on differentiated keratocytes from KC iPSC also showed that *FGFR2* gene expression was downregulated by 2-fold (Fig. 5E) and was supporting the RNA-Seq data. Taken together, our data and the data from the FGFR2 knockout mouse model[69] provide evidence that FGFR2 downregulation could have a significant impact on the development of KC.

In order to understand the mechanism and function of the FGFR2 downregulation, we differentiated the iPSC in the

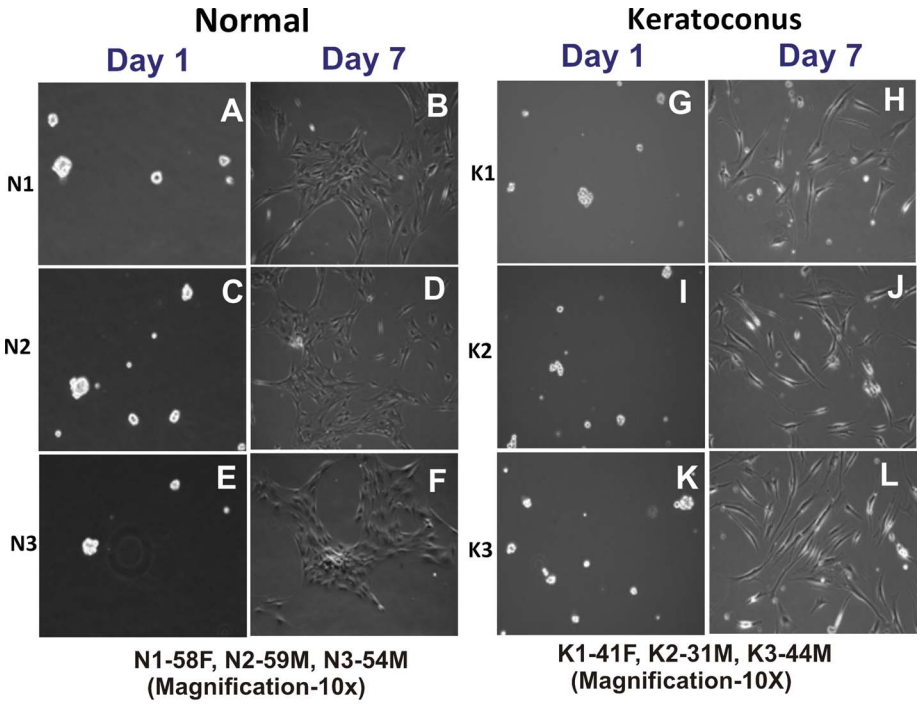

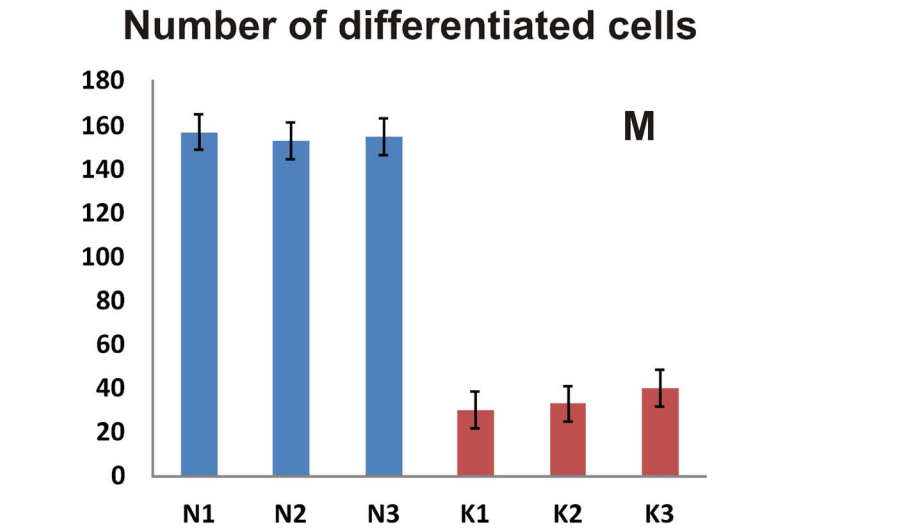

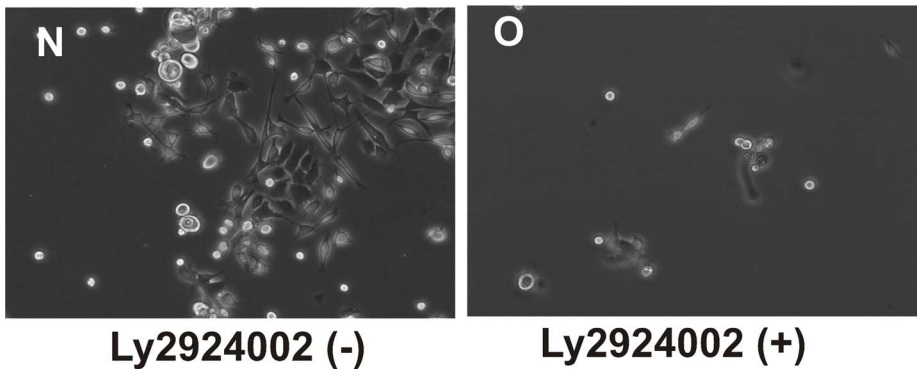

Figure 7. Proliferation of differentiated keratocytes. (**A**, **C**, **E**) Three normal corneal iPSC in differentiating media (58-year-old female, 59- and 54-year-old males, denoted as N1, N2, and N3, respectively). (**B**, **D**, **F**) Normal iPSC differentiation and cell proliferation. (**G**, **I**, **K**) Three keratoconus iPSC in differentiating media (41-year-old female, 31- and 44-year-old males, denoted as K1, K2, and K3, respectively). (**H**, **J**, **L**) Keratoconus iPSC differentiation and cell proliferation. Differentiation and proliferation were affected in KC iPSC-derived keratocytes. (**M**) Quantification of number of differentiated cells. (**N**, **O**) Effects of inhibition of Pi3 kinase by LY2924002. (**N**) Differentiation of normal stem cells in absence of the inhibitor, and (**O**) in the presence of the inhibitor. Pi3 kinase inhibition severely affects differentiation and proliferation of normal iPSC-derived keratocytes.

Investigative Ophthalmology & Visual Science

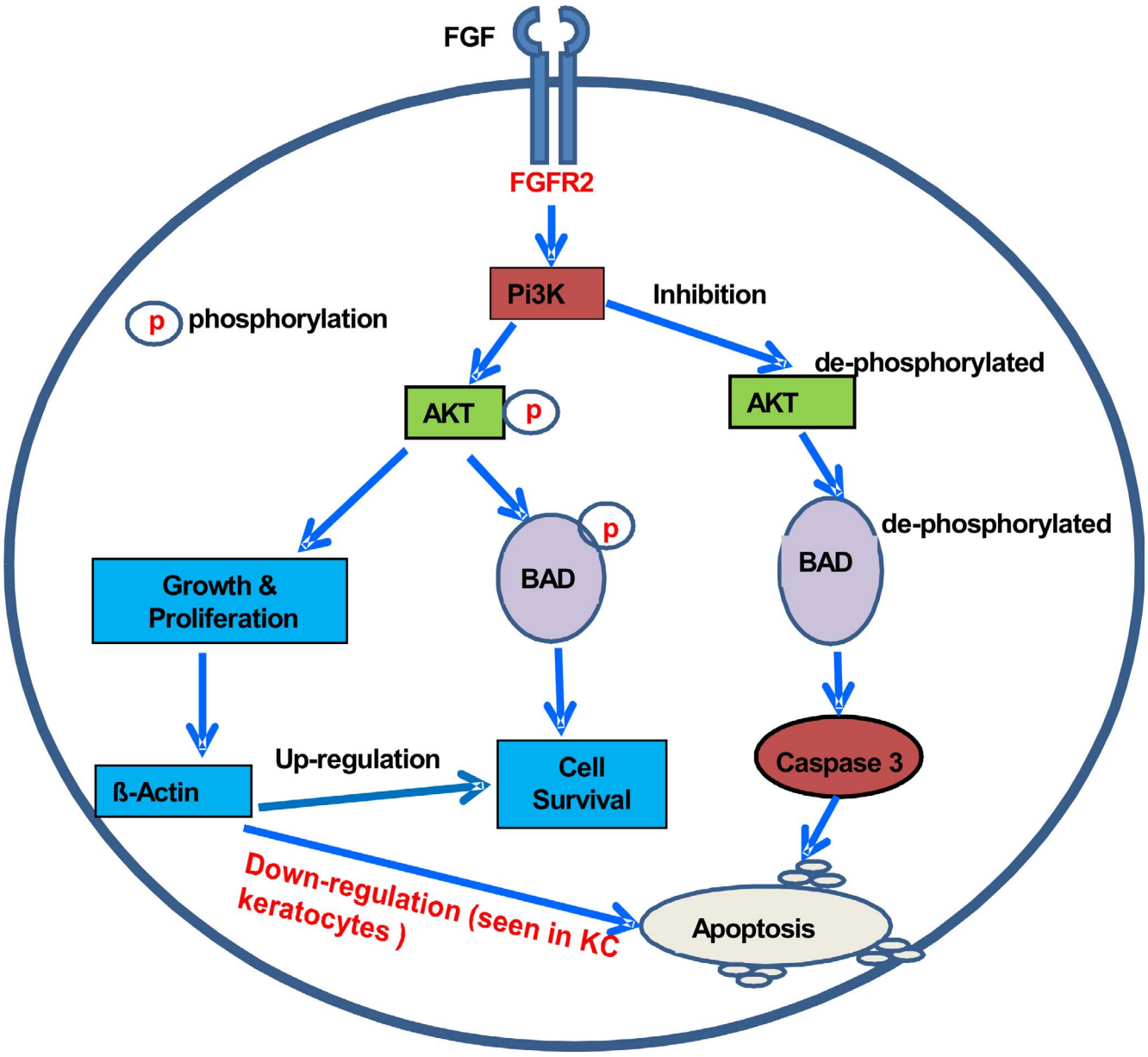

FIGURE 8. A proposed model of signaling pathway in KC cornea that leads to keratocyte apoptosis during KC. It shows the FGF signal transduction that results in the phosphorylation of AKT leading to growth and proliferation, and is mediated through BAD phosphorylation. When this signal transduction is inhibited, it leads to cell apoptosis. This could be potential mechanism for keratocytes apoptosis in keratoconus cornea.

presence of two different growth factors; FGF2 and insulin. Earlier studies have shown that keratocytes cultured in the media containing FGF2 have a fibroblastic phenotype, whereas with media-containing insulin has a dendritic morphology, but they both express keratocan, a marker for corneal keratocytes.[70,71] Our results also showed a similar effect in the presence of insulin and FGF2, which expressed keratocan (marker for keratocytes), but the cells showed a spindle phenotype (Fig. 6). We have shown that iPSC generated from both KC and normal have the potential to differentiate to keratocytes when cultured in the presence of differentiating media. But when keratocytes from KC iPSC were maintained in differentiating media for 7 days, the cell proliferation was inhibited compared with those from normal corneas (Fig. 7M). Because KC iPSC showed that cells differentiated into keratocytes with keratocan as a positive marker for differentiation, it could be that KC cells fail to proliferate even in the presence of mitogen. The RNA-Seq data (Supplementary Table S1) also show that KC iPSC have an altered cell cycle. Taking together, FGFR2 downregulation could inhibit the proliferation of cells as seen in KC. Phosphorylation of FGFR triggers several signaling cascades, of which are the RAS-RAF-mitogen activated protein kinase (MEK)-extracellular regulated kinase (ERK pathway), the phosphatidyl-inositol 3-kinase (PI3K) pathway is involved directly or indirectly in JAK-STAT pathway.[72] Fibroblast growth factor and IGF pathways have a common downstream target molecule, Pi3K. By blocking this target with the specific inhibitor Ly292004, we showed that inhibition of Pi3K resulted in inhibition of cell growth and proliferation in normal cells (Fig. 7O). These results suggest that both of these pathways are affected in KC stromal keratocytes and that an inhibitor of the downstream target Pi3K in normal cells causes them to resemble the growth and proliferation of keratocytes

Investigative Ophthalmology & Visual Science

derived from KC. We have also shown earlier that when PI3K was inhibited using Ly292004, the growth and proliferation was affected in normal corneal fibroblast.[46]

Based on the results of this study, we have proposed a model for the disease process leading to KC (Fig. 8). In this model, we propose that the binding of ligands, (FGF2 to receptor tyrosine kinase [RTK]) leads to receptor activation through autophosphorylation. On binding of growth factors to receptor tyrosine kinase (FGFR2), the signals are transduced through Pi3K that results in the phosphorylation of the downstream target, the serine-threonine kinase AkT. The AkT phosphorylation acts as a survival signal, resulting in the phosphorylation of Bcl-2-associated death promoter (BAD),[73] thus suppressing apoptosis and promoting cell survival. Alternatively, when AKT phosphorylation is inhibited, apoptosis is promoted, thus preventing the phosphorylation of BAD, a proapoptotic factor. In series of events, where phosphorylated BAD binds to BCL-X_L or BCL-2, suppress survival signals by inducing homodimer or hetrodimer formation, leading to caspase 3–induced keratocyte apoptosis.

Acknowledgments

The authors thank the Alabama Eye Bank for providing normal corneas for the study and also thank the technical assistance received from Heflin Genomics core facility (David Crossman, PhD) at the University of Alabama at Birmingham (Birmingham, AL, USA).

Supported by National Keratoconus Foundation (NKCF), Core Grant P30 EY003039 to Vision Science Research Center (VSRC), University of Alabama at Birmingham.

Disclosure: **R. Joseph**, None; **O.P. Srivastava**, None; **R.R. Pfister**, None

References

1. Kao WWY, Liu CY. Roles of lumican and keratocan on corneal transparency. *Glycoconj J*. 2002;19:275–285.
2. Chakravarti S, Magnuson T, Lass JH, Jepsen KJ, LaMantia C, Carroll H. Lumican regulates collagen fibril assembly: skin fragility and corneal opacity in the absence of lumican. *J Cell Biol*. 1998;141:1277–1286.
3. Chakravarti S, Petroll WM, Hassell JR, et al. Corneal opacity in lumican-null mice: defects in collagen fibril structure and packing in the posterior stroma. *Invest Ophthalmol Vis Sci*. 2000;41:3365–3373.
4. Kaldaawy RM, Wagner, J, Chig S, Seigel GM. Evidence of apoptotic death in keratoconus. *Cornea*. 2002;21:206–209.
5. Niederer RL, Perumal D, Sherwin T, McGhee CNJ. Laser scanning in vivo confocal microscopy reveals reduced innervation and reduction in cell density in all layers of the keratoconic cornea. *Invest Ophthalmol Vis Sci*. 2008;49: 2964–2970.
6. Kim W-J, Rabinowitz YS, Meisler DM, Wilson SE. Keratocyte apoptosis associated with keratoconus. *Exp Eye Res*. 1999;69: 475–481.
7. Lee J-E, Oum BS, Choi HY, Lee SU, Lee JS. Evaluation of differentially expressed genes identified in keratoconus. *Mol Vis*. 2009;15:2480–2487.
8. Mikami T, Meguro A, Teshigawara T, Takeuchi M, Uemoto R, Kawagoe T, et al. Interleukin 1 beta promoter polymorphism is associated with keratoconus in a Japanese population. *Mol Vis*. 2013;19:845–851.
9. Foster J, Wu W-H, Scott S-G, et al. Transforming growth factor β and insulin signal changes in stromal fibroblasts of individual keratoconus patients. *PLoS One*. 2014;9:e106556.
10. Martin GR. Isolation of a pluripotent cell line from early mouse embryos cultured in medium conditioned by teratocarcinoma stem cells. *Proc Natl Acad Sci*. 1981;78:7634–7638.
11. Joseph R, Srivastava OP, Pfister RR. Downregulation of β-actin gene and human antigen R in human keratoconus. *Invest Ophthalmol Vis Sci*. 2012;53:4032–4041.
12. Thomson JA. Embryonic stem cell lines derived from human blastocysts. *Science*. 1998;282:1145–1147.
13. Yamanaka S. Induced pluripotent stem cells: past, present, and future. *Cell Stem Cell*. 2012;10:678–684.
14. Maherali NSR, Xie W, Utikal J, et al. Directly reprogrammed fibroblasts show global epigenetic remodeling and widespread tissue contribution. *Cell Stem Cell*. 2007;1:55–70.
15. Wernig M, Meissner A, Foreman R, et al. In vitro reprogramming of fibroblasts into a pluripotent ES-cell-like state. *Nature*. 2007;448:318–324.
16. Lowry WE, Richter L, Yachechko R, et al. Generation of human induced pluripotent stem cells from dermal fibroblasts. *Proc Natl Acad Sci*. 2008;105:2883–2888.
17. Park I-H, Arora N, Huo H, et al. Disease-specific induced pluripotent stem (iPS) cells. *Cell*. 2008;134:877–886.
18. Zhou L, Wang W, Liu Y, et al. Differentiation of induced pluripotent stem cells of swine into rod photoreceptors and their integration into the retina. *Stem Cells*. 2011;29:972–980.
19. Chien Y, Liao Y-W, Liu D-M, et al. Corneal repair by human corneal keratocyte-reprogrammed iPSCs and amphiphatic carboxymethyl-hexanoyl chitosan hydrogel. *Biomaterials*. 2012;33:8003–8016.
20. Chan AA, Hertsenberg AJ, Funderburgh ML, et al. Differentiation of human embryonic stem cells into cells with corneal keratocyte phenotype. *PLoS One*. 2013;8:e56831.
21. Takahashi K, Tanabe K, Ohnuki M, et al. Induction of pluripotent stem cells from adult human fibroblasts by defined factors. *Cell*. 2007;131:861–872.
22. Chin MH, Pellegrini M, Plath K, Lowry WE. Molecular analyses of human induced pluripotent stem cells and embryonic stem cells. *Cell Stem Cell*. 2010;7:263–269.
23. Hawkins RD, Hon GC, Lee LK, et al. Distinct epigenomic landscapes of pluripotent and lineage-committed human cells. *Cell Stem Cell*. 2010;6:479–491.
24. Dimos JT, Rodolfa KT, Niakan KK, Weisenthal LM, Mitsumoto H, Chung W, et al. Induced pluripotent stem cells generated from patients with ALS can be differentiated into motor neurons. *Science*. 2008;321:1218–1221.
25. Maehr R, Chen S, Snitow M, et al. Generation of pluripotent stem cells from patients with type 1 diabetes. *Proc Natl Acad Sci*. 2009;106:15768–15773.
26. Soldner F, Hockemeyer D, Beard C, et al. Parkinson's disease patient-derived induced pluripotent stem cells free of viral reprogramming factors. *Cell*. 2009;136:964–977.
27. Chamberlain SJ, Chen P-F, Ng KY, et al. Induced pluripotent stem cell models of the genomic imprinting disorders Angelman and Prader–Willi syndromes. *Proc Natl Acad Sci*. 2010; 107:17668–17673.
28. Urbach A, Bar-Nur O, Daley GQ, Benvenisty N. Differential modeling of fragile X syndrome by human embryonic stem cells and induced pluripotent stem cells. *Cell Stem Cell*. 2010; 6:407–411.
29. Ebert AD, Yu J, Rose FF, et al. Induced pluripotent stem cells from a spinal muscular atrophy patient. *Nature*. 2009;457: 277–280.
30. Ku S, Soragni E, Campau E, et al. Friedreich's ataxia induced pluripotent stem cells model intergenerational GAA•TTC triplet repeat instability. *Cell Stem Cell*. 2010;7:631–637.
31. Itzhaki I, Maizels L, Huber I, et al. Modelling the long QT syndrome with induced pluripotent stem cells. *Nature*. 2011; 471:225–229.

32. Liu L, Rando TA. Manifestations and mechanisms of stem cell aging. *J Cell Biol*. 2011;193:257–266.
33. Zhang Z, Gao Y, Gordon A, Wang ZZ, Qian Z, Wu W-S Efficient generation of fully reprogrammed human iPS cells via polycistronic retroviral vector and a new cocktail of chemical compounds. *PLoS One*. 2011;6:e26592.
34. Tsuchihara K, Suzuki Y, Wakaguri H, et al. Massive transcriptional start site analysis of human genes in hypoxia cells. *Nucleic Acids Res*. 2009;37:2249–2263.
35. Cloonan N, Forrest ARR, Kolle G, et al. Stem cell transcriptome profiling via massive-scale mRNA sequencing. *Nat Meth*. 2008; 5:613–619.
36. Morin RD, O'Connor MD, Griffith M, et al. Application of massively parallel sequencing to microRNA profiling and discovery in human embryonic stem cells. *Genome Res*. 2008;18:610–621.
37. Nagalakshmi U, Wang Z, Waern K, et al. The transcriptional landscape of the yeast genome defined by RNA sequencing. *Science*. 2008;320:1344–1349.
38. Shendure J, Ji H. Next-generation DNA sequencing. *Nat Biotech*. 2008;26:1135–1145.
39. Wilhelm BT, Marguerat S, Watt S, et al. Dynamic repertoire of a eukaryotic transcriptome surveyed at single-nucleotide resolution. *Nature*. 2008;453:1239–1243.
40. Wang Z, Gerstein M, Snyder M. RNA-Seq: a revolutionary tool for transcriptomics. *Nat Rev Genet*. 2009;10:57–63.
41. Carey BW, Markoulaki S, Hanna J, et al. Reprogramming of murine and human somatic cells using a single polycistronic vector. *Proc Natl Acad Sci*. 2009;106:157–162.
42. Trapnell C, Pachter L, Salzberg SL. TopHat: discovering splice junctions with RNA-Seq. *Bioinformatics*. 2009;25:1105–1111.
43. Langmead B, Trapnell C, Pop M, Salzberg SL. Ultrafast and memory-efficient alignment of short DNA sequences to the human genome. *Genome Biol*. 2009;10:R25.
44. Trapnell C, Roberts A, Goff L, et al. Differential gene and transcript expression analysis of RNA-seq experiments with TopHat and Cufflinks. *Nat Protocols*. 2012;7:562–578.
45. Trapnell C, Williams BA, Pertea G, et al. Transcript assembly and quantification by RNA-Seq reveals unannotated transcripts and isoform switching during cell differentiation. *Nat Biotech*. 2010;28:511–515.
46. Joseph R, Srivastava OP, Pfister RR. Downregulation of β-actin and its regulatory gene HuR affect cell migration of human corneal fibroblasts. *Mol Vis*. 2014;20:593–605.
47. Park I-H, Lerou PH, Zhao R, Huo H, Daley GQ. Generation of human-induced pluripotent stem cells. *Nat Protocols*. 2008;3: 1180–1186.
48. Devine MJ, Ryten M, Vodicka P, et al. Parkinson's disease induced pluripotent stem cells with triplication of the α-synuclein locus. *Nat Commun*. 2011;2:440.
49. Israel MA, Yuan SH, Bardy C, et al. Probing sporadic and familial Alzheimer's disease using induced pluripotent stem cells. *Nature*. 2012;482:216–220.
50. Yagi T, Ito D, Okada Y, et al. Modeling familial Alzheimer's disease with induced pluripotent stem cells. *Hum Mol Genet*. 2011;20:4530–4539.
51. Kondo T, Asai M, Tsukita K, et al. Modeling Alzheimer's disease with iPSCs reveals stress phenotypes associated with intracellular Aβ and differential drug responsiveness. *Cell Stem Cell*. 2013;12:487–496.
52. Brennand KJ, Simone A, Jou J, et al. Modelling schizophrenia using human induced pluripotent stem cells. *Nature*. 2011; 473:221–225.
53. Takahashi K, Yamanaka S. Induction of pluripotent stem cells from mouse embryonic and adult fibroblast cultures by defined factors. *Cell*. 2006;126:663–676.
54. Chin MH, Mason MJ, Xie W, et al. Induced pluripotent stem cells and embryonic stem cells are distinguished by gene expression signatures. *Cell Stem Cell*. 2009;5:111–123.
55. Ji J, Ng SH, Sharma V, et al. Elevated coding mutation rate during the reprogramming of human somatic cells into induced pluripotent stem cells. *Stem Cells*. 2012;30:435–440.
56. Ozsolak F, Milos PM. RNA sequencing: advances, challenges and opportunities. *Nat Rev Genet*. 2011;12:87–98.
57. Li X, Bykhovskaya Y, Canedo ALC, et al. Genetic association of COL5A1 variants in keratoconus patients suggests a complex connection between corneal thinning and keratoconusassociation of COL5A1 variants in keratoconus. *Invest Ophthalmol Vis Sci*. 2013;54:2696–2704.
58. Dong M, How T, Kirkbride KC, et al. The type III TGF-β receptor suppresses breast cancer progression. *J Clin Invest*. 2007;117:206–217.
59. Hempel N, How T, Dong M, Murphy SK, Fields TA, Blobe GC. Loss of betaglycan expression in ovarian cancer: role in motility and invasion. *Cancer Res*. 2007;67:5231–5238.
60. Gautreau A, Poullet P, Louvard D, Arpin M. Ezrin, a plasma membrane–microfilament linker, signals cell survival through the phosphatidylinositol 3-kinase/Akt pathway. *Proc Natl Acad Sci*. 1999;96:7300–7305.
61. van de Weerdt BC, Medema RH. Polo-like kinases: a team in control of the division. *Cell Cycle*. 2006;5:853–864.
62. Lu Y, Vitart V, Burdon KP, et al. Genome-wide association analyses identify multiple loci associated with central corneal thickness and keratoconus. *Nat Genet*. 2013;45:155–163.
63. Sahebjada S, Schache M, Richardson AJ, Snibson G, Daniell M, Baird PN. Association of the hepatocyte growth factor gene with keratoconus in an Australian population. *PLoS One*. 2014;9:e84067.
64. Nielsen K, Birkenkamp-Demtröder K, Ehlers N, Orntoft TF. Identification of differentially expressed genes in keratoconus epithelium analyzed on microarrays. *Invest Ophthalmol Vis Sci*. 2003;44:2466–2476.
65. Jun AS, Cope L, Speck C, et al. Subnormal cytokine profile in the tear fluid of keratoconus patients. *PLoS One*. 2011;6: e16437.
66. Sutton G, Madigan M, Roufas A, McAvoy J. Secreted frizzled-related protein 1 (SFRP1) is highly upregulated in keratoconus epithelium: a novel finding highlighting a new potential focus for keratoconus research and treatment. *Clin Exp Ophthalmol*. 2010;38:43–48.
67. Kennedy SG, Wagner AJ, Conzen SD, et al. The PI 3-kinase/Akt signaling pathway delivers an anti-apoptotic signal. *Genes Dev*. 1997;11:701–713.
68. Wilson SE, Walker JW, Chwang EL, He YG. Hepatocyte growth factor, keratinocyte growth factor, their receptors, fibroblast growth factor receptor-2, and the cells of the cornea. *Invest Ophthalmol Vis Sci* 1993;34:2544–2561.
69. Zhang J, Upadhya D, Lu L, Reneker LW. Fibroblast growth factor receptor 2 (FGFR2) is required for corneal epithelial cell proliferation and differentiation during embryonic development. *PLoS One*. 2015;10:e0117089.
70. Musselmann K, Alexandrou B, Kane B, Hassell JR. Maintenance of the keratocyte phenotype during cell proliferation stimulated by insulin. *J Biol Chem*. 2005;280:32634–32639.
71. Long CJ, Roth MR, Tasheva ES, et al. Fibroblast growth factor-2 promotes keratan sulfate proteoglycan expression by keratocytes in vitro. *J Biol Chem*. 2000;275:13918–13923.
72. Schlessinger J. Cell signaling by receptor tyrosine kinases. *Cell*. 2000;103:211–225.
73. Datta SR, Dudek H, Tao X, et al. Akt phosphorylation of BAD couples survival signals to the cell-intrinsic death machinery. *Cell*. 1997;91:231–241.